

# High-Speed Full-Range Imaging with Harmonic Detection Swept-Source Optical Coherence Tomography

Chuanyong Huang, Steven M. Massick, Kristen A. Peterson and Andrei B. Vakhtin  
Southwest Sciences, Inc., 1570 Pacheco St., Suite E-11, Santa Fe, NM, USA 87505  
peterson@swsciences.com



## Abstract

High-speed full-range imaging using harmonically detected Fourier domain OCT is demonstrated using 1300 nm broadband swept light source. While maintaining the imaging performance of the original swept source instrument, this harmonic detection swept source optical coherence tomography (HD SSOCT) system exhibits high sensitivity, large dynamic range, and excellent complex conjugate rejection suitable for real-time clinical imaging.

## 1. Introduction

Swept source optical coherence tomography (SSOCT) is attractive for clinical OCT applications because of its high sensitivity and imaging speed. However, a limiting factor of all Fourier domain OCT methods, including SSOCT, is the complex conjugate ambiguity due to Fourier transform of real-valued data; the image is symmetric with respect to the zero plane of the interferometer. Only half of the imaging depth range is useful in practice to avoid overlapping "mirror images." Resolving the complex conjugate ambiguity doubles the available imaging depth range by allowing the interferometer zero plane to be within the sample.

Importantly, HD-SSOCT acquires complex spectral interferograms. The imaginary and real components of the interferogram are simultaneously acquired as the first and second harmonics of a MHz phase-modulated signal. Each complex spectral interferogram is measured directly for a single A-scan without needing to measure consecutive A-scans at differing phase. The real and imaginary components are obtained during the acquisition of a single spectral interferogram and a single inverse complex FFT provides the depth profile free of complex conjugate, DC and auto-correlation artifacts. This is possible because the phase modulation frequency is significantly higher than the A-scan rate. Furthermore, the high phase modulation frequency makes this approach less sensitive to phase noise in the interferometer. HD-SSOCT provides high speed imaging in a simple, robust configuration suitable for clinical applications.

## 2. Mathematical Basis of HD-SSOCT

Consider a sample with only one back-scattering surface (e.g., a mirror). The spectral interferogram at the output of a phase modulated interferometer is:

$$I_S(k, t) = I_R(k) + I_S(k) + 2 [I_R(k) I_S(k)]^{1/2} \cos[\Delta\phi_S(k) + \phi_0(k, t)] \quad (1)$$

where  $k$  is the wavenumber ( $k = 2\pi/\lambda$ );  $t$  is time;  $I_R(k)$  and  $I_S(k)$  are the light intensities in the reference and the sample arms of the interferometer, respectively;  $\Delta\phi_S(k)$  is the phase delay corresponding to the sample ( $\Delta\phi_S(k) = 2k\Delta z$ , where  $\Delta z$  is the optical path difference between the sample and the reference mirror);  $\phi_0(k, t)$  is time-dependent sinusoidal phase modulation term  $\phi_0(k, t) = a_m(k) \sin \omega_m t$ , where  $\omega_m = 2\pi f_m$ ,  $f_m$  is the phase modulation frequency, and  $a_m(k)$  is the phase modulation amplitude.

Expanding the last term on the right side of Eq. (1) into series of Bessel functions ( $J_0, J_1, J_2, \dots$ ), the signals demodulated at the first ( $H_1$ ) and the second ( $H_2$ ) harmonics of the modulation frequency represent the imaginary and real parts of the complex spectral interferogram, respectively.

$$H_1[k, \Delta\phi_S(k)] = -4 J_1[a_m(k)] [I_R(k) I_S(k)]^{1/2} \sin \Delta\phi_S(k) \quad (2)$$

$$H_2[k, \Delta\phi_S(k)] = 4 J_2[a_m(k)] [I_R(k) I_S(k)]^{1/2} \cos \Delta\phi_S(k) \quad (3)$$

The complex inverse Fourier transform can be applied to the complex interferogram to convert it into the time domain profile that is free from complex conjugate ambiguity and also the dc and autocorrelation terms:

$$\tilde{f}(z) = \mathcal{F}^{-1}\{\beta H_2[k, \Delta\phi_S(k)] - i H_1[k, \Delta\phi_S(k)]\} \quad (4)$$

According to Eqs (2) and (3), the scaling coefficient  $\beta$  is equal to

$$\beta = J_1[a_m(k)]/J_2[a_m(k)] \quad (5)$$

and depends only on the modulation amplitude  $a_m$ . Generally,  $a_m$  is wavelength dependent which can be corrected for in post processing. In these experiments we found a linear assumption sufficient:

$$a_m(k) = a_m(k_0)k/k_0 \quad (6)$$

where  $a_m(k_0)$  is the modulation amplitude at wavenumber  $k_0$ , and  $k_0$  is the center wavenumber of the spectral window.

The modulation amplitude does not need to be known accurately. It ( $a_m$  or  $\beta$ ) can be treated as an adjustable parameter. Alternatively, the modulation amplitude can be experimentally adjusted to optimize the complex conjugate rejection. This initial setup has to be performed *only once* for a given set of experimental conditions.

## 3. Harmonically Detected SSOCT

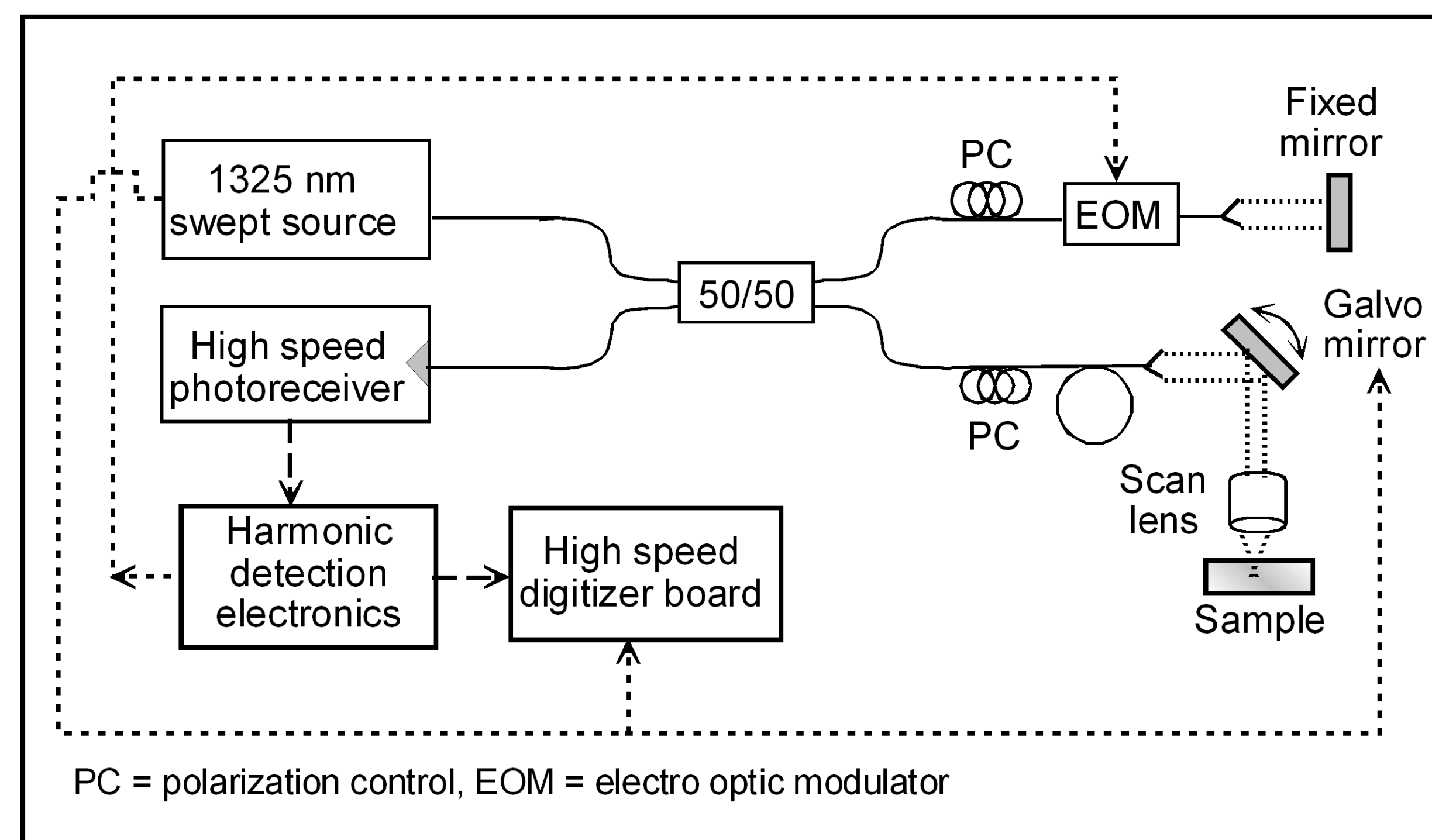


Figure 1. Schematic of the HD-SSOCT instrument

The photodiode signal is demodulated by the "harmonic detection electronics" (Fig. 2) at the first harmonic (30 MHz) and second harmonic (60 MHz) of the phase modulation frequency, providing the imaginary and real spectral interferograms, respectively. These signals are simultaneously digitized using a high speed digitizer board.

## 4. Harmonic Detection Electronics

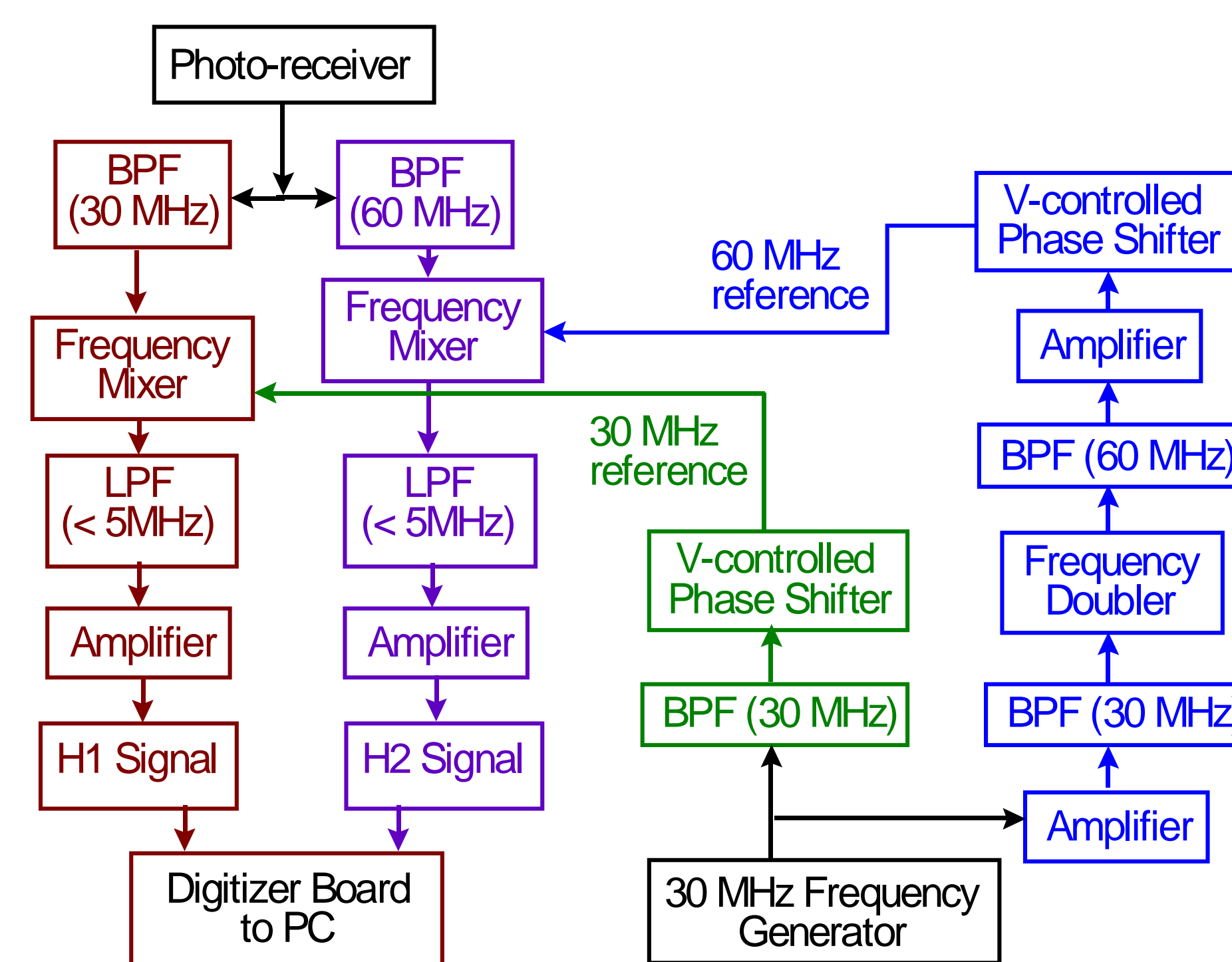


Figure 2. Schematic of the harmonic detection electronics

## 5. Instrument Performance

Specification	HD-SSOCT Instrument	Thorlabs OCS1300SS SSOCT Instrument
Sensitivity	110 dB	108 dB
Dynamic range	50 – 55 dB	Not available
Lateral resolution in air	13 1 $\mu\text{m}$	13 $\mu\text{m}$
Axial resolution in air	12 1 $\mu\text{m}$	12 $\mu\text{m}$
A-scan rate	16 kHz	16 kHz
B-scan rate (Hz) (512 A-scans/frame)	$\geq 25$ Hz	25 Hz
Complex conjugate rejection	$\geq 50$ dB	Not applicable

The Thorlabs system values are from ThorLabs publications & it uses the same light source and a similar optical arrangement to the HD-SSOCT, but a dual-balanced detection system to remove common noise, dc and autocorrelation artifacts. The Thorlabs instrument does not provide complex conjugate rejection. Lateral resolution is given for the LSM02 scan lens.

## 6. Images Obtained by HD-SSOCT

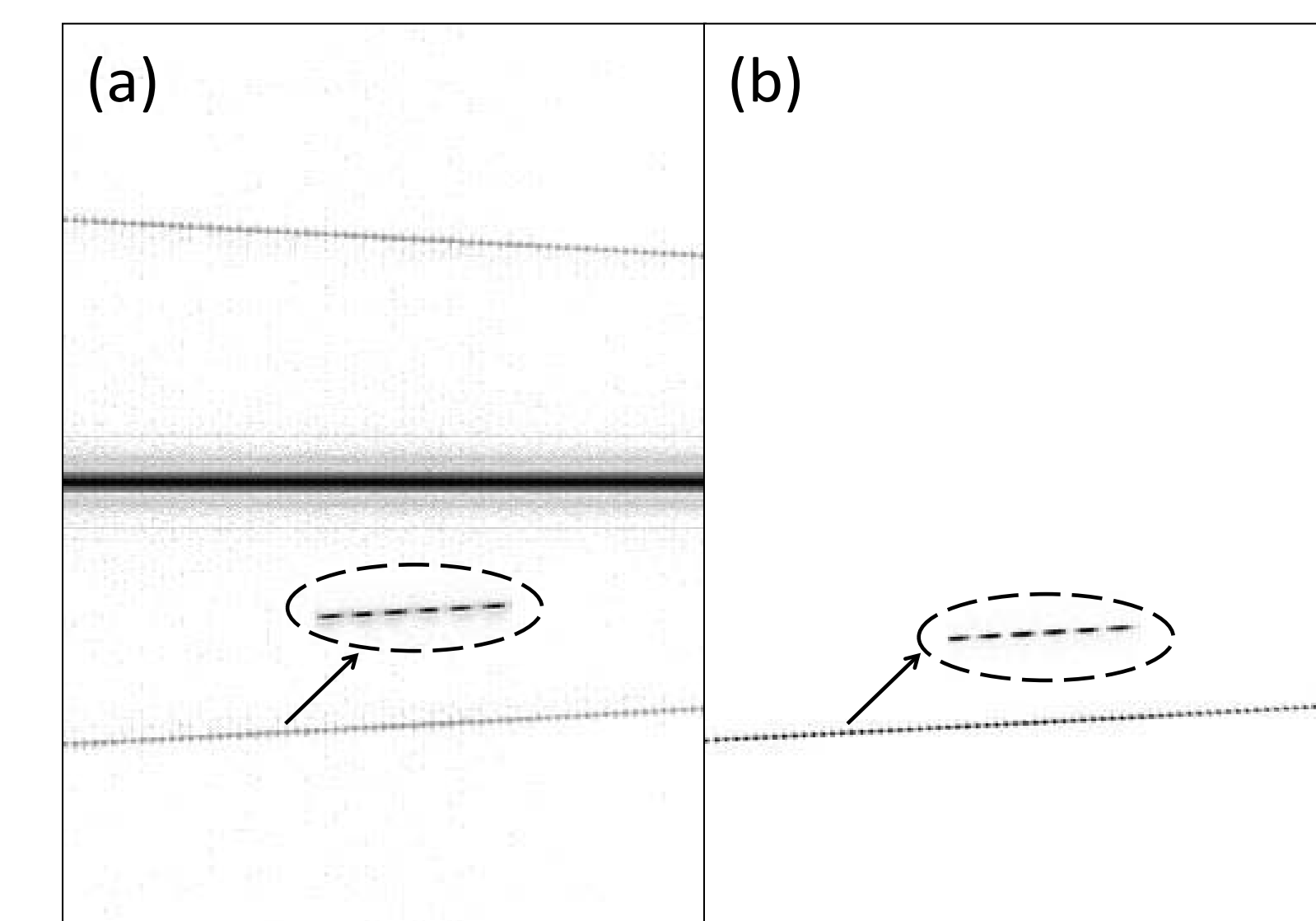


Figure 3. Images of a 40 line pair/mm Ronchi grating using normal swept source OCT (a); and using harmonic detection which removes the artifacts (b). Inserts show a magnified region of the image demonstrating the resolution.

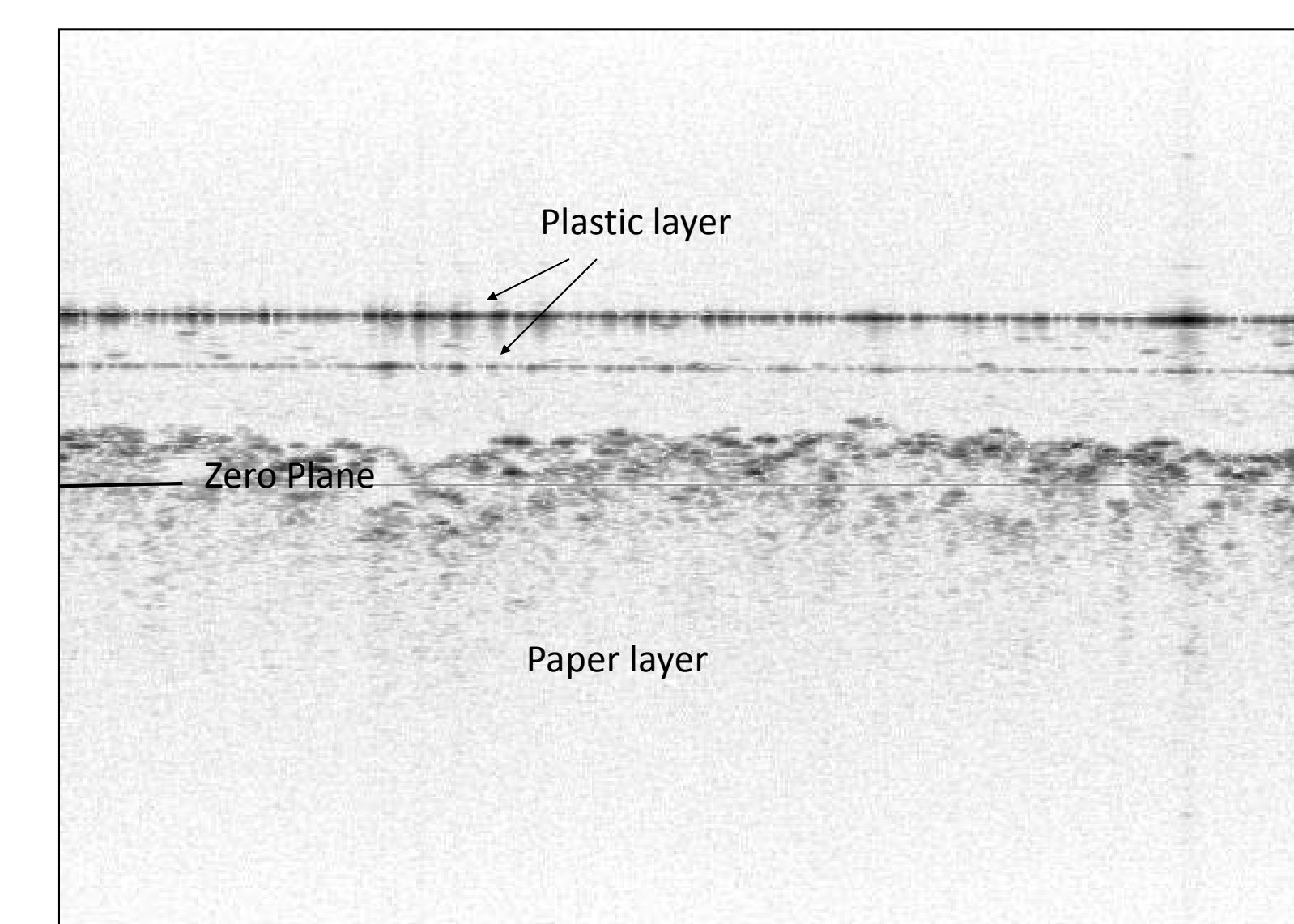


Figure 4. HD-SSOCT image of a plastic coated paper card. The zero plane is within the sample. There is no complex conjugate artifact confounding the image.

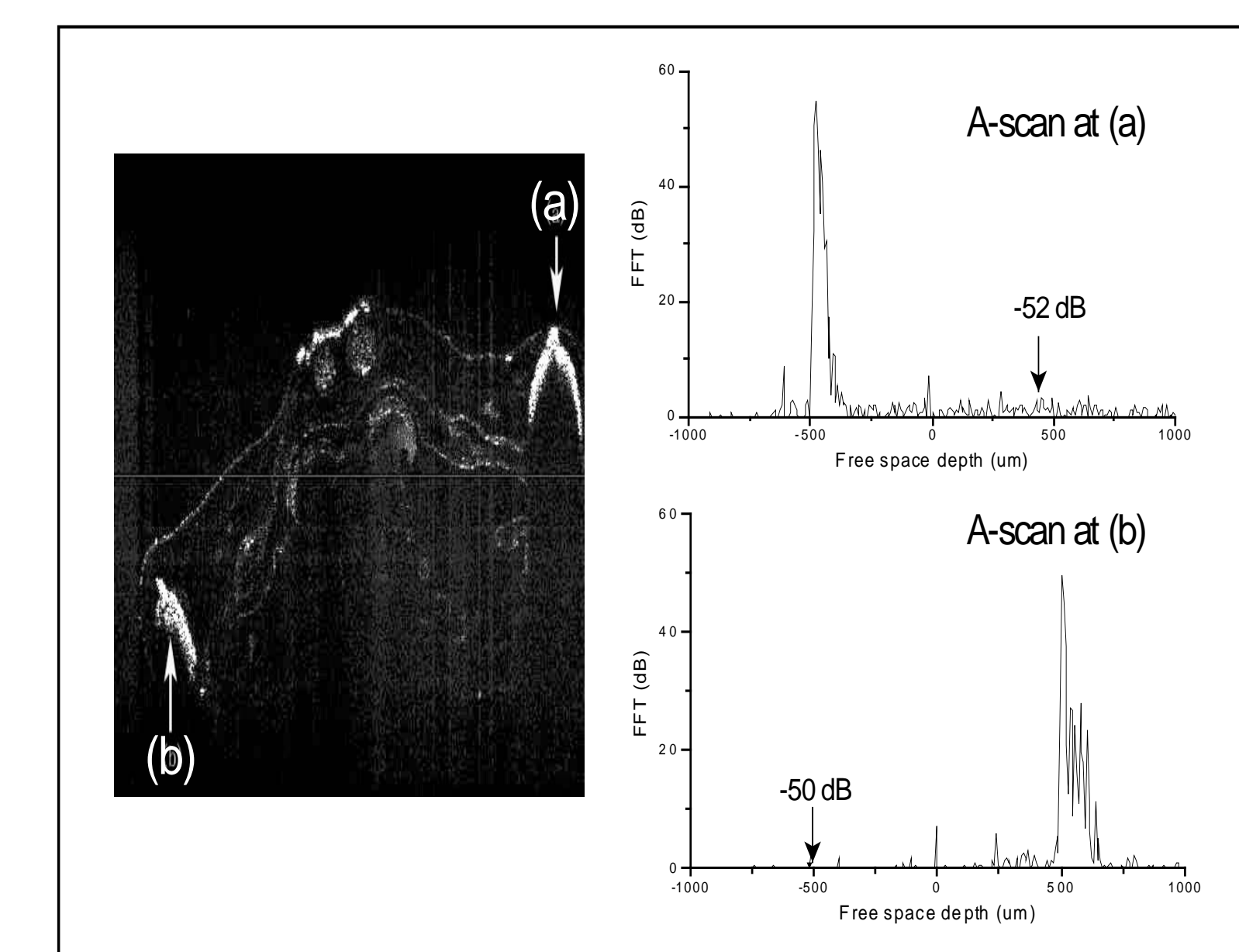


Figure 5. HD-SSOCT cross-sectional image from the head region of a *X. tropicalis* tadpole (left) and corresponding A-scans from points (a) and (b). The bright features at (a) and (b) are from the eyes and nearly saturate the detector. The white horizontal line in the image indicates the zero plane. Rejection is  $\geq 50$  dB.

## 7. Summary

Harmonic detection provides excellent rejection of artifacts in SSOCT while providing high sensitivity and dynamic range in a real-time, video rate system. The complex conjugate rejection ratio of  $\geq 50$  dB is better than the 30 – 40 dB rejection typically reported for B-M mode scanning or piezoelectric fiber stretcher approaches. Harmonic detection is easily applied to SSOCT, and our use of commercial components of an SSOCT instrument (light source, digitizer board, optics and scanner) show that, upon redesign of the electronics into a compact package, harmonic detection can be readily incorporated into a commercial instrument.

### Previous Publications:

- Vakhtin A. B., Peterson K. A. and Kane D. J., "Demonstration of complex-conjugate-resolved harmonic Fourier domain OCT imaging of biological samples," *Applied Optics* 46, 3870-3877 (2007).
- Vakhtin, A. B., Kane, D. J., and Peterson K. A. "Method and Apparatus for Full Phase Interferometry," Southwest Sciences, Inc., US Patent 7,394,546 (2008).
- Vakhtin A. B., Peterson K. A. and Kane D. J., "Real-time video-rate harmonically detected Fourier domain optical coherence tomography," *Proc. SPIE*, 6847, 6847R1-5 (2008).

This work is supported by the NIH, NHLBI under SBIR Grant R44HL90627.